

RAINDROP COMPLEMENT BASED ON EPIPOLAR GEOMETRY AND SPATIOTEMPORAL PATCHES

Kyohei Nomoto, Fumihiko Sakaue and Jun Sato
Nagoya Institute of Technology, Gokiso, Showa, Nagoya 466-8555, Japan

Keywords: Auto-epipolar geometry, Spatiotemporal image, Image in-painting.

Abstract: In this paper, we propose detection and complement of raindrops on mirrors and windows onto cars. Raindrops on windows and mirrors disturb view of drivers. In general, they were removed using wiper and special devices. However, the devices cannot be used for general case. In our proposed method, images of mirrors and windows are taken by camera and raindrops are complemented on the images, virtually. The method is based on auto-epipolar geometry and concept of spatiotemporal image. By using the method, we can observe clear windows and mirrors only if we can take them by camera.

1 INTRODUCTION

Recently, multiple cameras are equipped on vehicles for various kinds of purposes. These vehicle cameras obtain lots of information which can help drivers. The extracted information is presented to drivers in various ways. For example, virtual dead angle images of driver's view can be synthesized by using multiple vehicle cameras. From these images, drivers can observe pedestrians and obstacles in dead angles, and can avoid car accidents. Many other applications can be considered for assisting vehicle drivers by using vehicle cameras. In this paper, we consider a system which supports drivers in rainy days by using vehicle cameras.

In rainy days, raindrops on side mirrors and windows disturb drivers view as shown in Fig.1 (a). For the safety driving, these raindrops should be removed as shown in Fig.1 (b). Although the raindrops on front windows can be removed by using wipers, there is no wipers for raindrops on side mirrors and side windows in general. Thus, we in this paper propose a method for removing these raindrops not in physical way but in virtual way. The proposed method can be applied to not only side mirrors and windows but also other windows and mirrors to obtain clear views without using wipers.

In our method, windows and mirrors are taken by cameras equipped on vehicles, and raindrops in images are removed by using the image in-painting technique. By using the proposed method, images without raindrops can be presented to vehicle drivers, and the

drivers can observe clear windows and mirrors.

In order to achieve raindrop removal, we have to extract raindrop areas in images and complement these areas. This is called image complement or image in-painting, and various methods have been proposed. Many others proposed image complement methods for static scenes viewed from static cameras (Efros and Freeman, 2001; Bertalmio et al., 2000; Bertalmio et al., 2001; Kang et al., 2002; Bertalmio et al., 2003; Matsushita et al., 2005; Shen et al., 2006; Wexler et al., 2007; Hase et al., 1999). However, these methods cannot be applied for vehicle cameras, since vehicle cameras are moving rapidly, and the scene changes continually. Furthermore, these methods cannot recover large image lack such as occlusions. Kuribayashi and others proposed image in-painting methods for moving cameras (Kuribayashi et al., 2009). However, these methods are limited to cameras whose motions are parallel to image planes. In this case, image motions are constant, and are parallel to each other. Thus, image in-painting is rather simple. In our case, camera motions, i.e. mirror motions, are not parallel to the image plane, and the image motions are not constant and vary depending on the 3D position of scene points.

To complement images taken under general translational cameras, we consider epipolar geometry in sequential images. In particular we consider the auto epipolar geometry, which provides us very strong constraints for complimenting images properly by using past sequential images.



Figure 1: Images which has raindrops and no raindrops.

2 EPIPOLAR GEOMETRY FOR TRANSLATING CAMERA

In this paper, we propose a method which enables us to detect and complement raindrops on mirrors and windows in images. In this method, we assume that the images are taken by a translational camera, which is a reasonable assumption for images taken by vehicle cameras.

If a static scene is observed by a moving camera, the relationship among sequential images taken by the moving camera can be described by the epipolar geometry. Furthermore, if there is no rotation in the camera motion, i.e. pure translation, the relationship among images can be described by the auto-epipolar geometry (Hartley and Zisserman, 2000). When the auto-epipolar geometry holds, epipoles and epipolar lines in two different images are equivalent to each other, and then, the epipolar geometry can be estimated very accurately. In this paper, we use the auto-epipolar geometry for efficient and stable image complement. In this section, we describe the detail of the auto-epipolar geometry.

2.1 Auto-epipolar Geometry on Translational Cameras

In general, the relationship between corresponding points, \mathbf{x} and \mathbf{x}' , in two different views can be described by the following epipolar equation:

$$\mathbf{x}'^T \mathbf{F} \mathbf{x} = 0 \quad (1)$$

where, \mathbf{F} is a 7 DOF rank 2 matrix called fundamental matrix. Note, in this paper, points and lines are represented by homogeneous coordinates.

Suppose we have a translational camera as shown in Fig. 2. The 3D points \mathbf{X}_i ($i = 1, \dots, N$) are projected to \mathbf{x}_i and \mathbf{x}'_i in two images, and epipolar lines \mathbf{l}_i and \mathbf{l}'_i go through these corresponding points. In this case, the auto epipolar geometry holds, and the fundamental matrix \mathbf{F} has only 2 DOF. Thus, the fundamental matrix can be estimated from only 2 corresponding points stably. In this case, epipoles and epipolar lines

are identical in two images. Thus, the epipolar line \mathbf{l}_i can simply be estimated by connecting corresponding points \mathbf{x}_i and \mathbf{x}'_i as follows:

$$\mathbf{l}_i = \mathbf{x}_i \times \mathbf{x}'_i \quad (2)$$

where, \times denotes a vector product. Furthermore, the epipole \mathbf{e} can be estimated as an intersection of epipolar lines as follows:

$$\mathbf{e} = \mathbf{l}_1 \times \mathbf{l}_2. \quad (3)$$

By using the epipole, the fundamental matrix \mathbf{F} is described as follows:

$$\mathbf{F} = [\mathbf{e}]_{\times} \quad (4)$$

where $[\cdot]_{\times}$ denotes a 3×3 skew symmetric matrix, which represents the vector product. Thus, the fundamental matrix can be estimated from minimum of two corresponding points. Since the DOF of the fundamental matrix is much smaller than that of general case, it can be estimated quite reliably from small number of corresponding points.

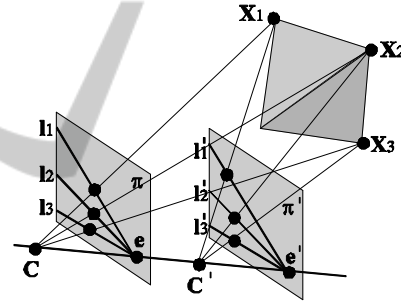


Figure 2: Auto-epipolar geometry on translating cameras.

2.2 Parallelization of Epipolar Lines

In the previous section, we described auto-epipolar geometry. Under general translational motions, the epipolar lines are not parallel to each other. Since efficient image processing can be accomplished when the epipolar lines are parallel to each other, we in this section consider parallelization of epipolar lines by using projective transformation.

The epipolar lines are intersected at an epipole, and thus, the epipolar lines become parallel to each other, if the epipole is moved to a point at infinity. Therefore, we estimate a projective transformation, which moves the epipole to an infinite point. Such projective transformation \mathbf{H} satisfies the following equation:

$$\lambda \begin{bmatrix} e_1 \\ e_2 \\ 0 \end{bmatrix} = \mathbf{H} \mathbf{e} \quad (5)$$

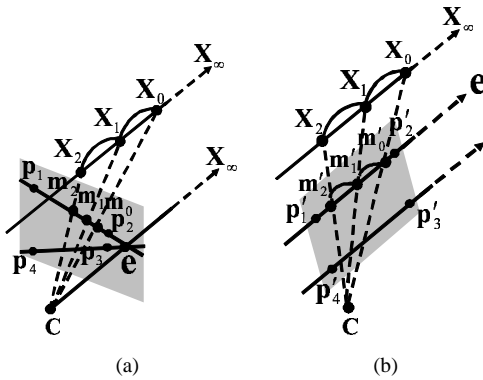


Figure 3: Parallelization of epipolar lines using 2D projective transformation. (a) shows a general translational camera, and (b) shows the camera after parallelization. The translational camera can be considered as a static camera which observe translational 3D points X_j . The parallelization of epipolar lines can be achieved by rotating the image plane so that it is parallel to the direction of translation.

where e_1 and e_2 denote the first and the second components of the epipole e . By using the transformation, all epipolar lines become parallel to each other. The transformation H implies image plane rotation, and the rotated image planes are parallel to the direction of camera translation as shown in Fig.3.

Figure 4 shows example of image parallelization. In this figure, a projective image distortion is eliminated by image parallelization. By using the transformed images, the image complement can be achieved efficiently as described in the next section.

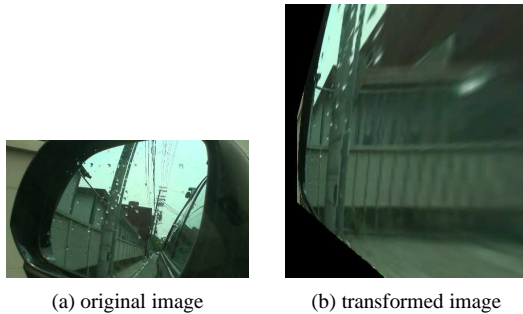


Figure 4: Exampe of image parallelization of a side mirror image. (a) shows an original image and (b) shows the image after parallelization of epipolar lines.

3 IMAGE COMPLEMENTS USING SPATIOTEMPORAL PATCHES

3.1 Complementation of Raindrop

In the previous section, we considered geometric

properties of sequential images captured from translational cameras and their parallelization. In this section, we propose an image complement method for parallelized sequential images. Although raindrops on windows and mirrors must be detected before image complement, we consider the image complement method before considering the raindrop detection method, since the raindrop detection method is based on image complement in our method.

In the sequential images of a camera mounted on a moving vehicle, image pixels occluded by raindrops can be observed in other frames. Thus, the occluded pixels can be inpainted by using image information in other frames. Wexler proposed image completion method for spatiotemporal images(Wexler et al., 2007). In their method, they considered not only current single frame, but also multiple sequential frames, and spatiotemporal patches are used for image completion. However, their method can only be applied to the scene taken by a fixed camera, and thus, it cannot be applied to image sequences taken by a translational camera. In order to inpaint images taken by translational cameras, we extend their method by using auto-epipolar geometry.

3.2 Image Complements using Spatiotemporal Images

Now, let us consider sequential images taken by a translational camera. As shown in section 2, the auto-epipolar geometry holds in this case. In this paper, we consider the sequential images as a spatiotemporal image as shown in Fig.5 (a). When the auto-epipolar geometry holds, epipolar lines and epipoles in sequential images are identical to each other. Thus, if we consider a slice along an epipolar line, we have the slice which represents image point motions in the translational camera as shown in Fig.5 (a). In this slice, the epipole does not move because of the auto-epipolar. The raindrops also do not move. On the other hand, background objects such as trees move on the epipolar lines as shown in Fig.5 (a). Furthermore, when images are parallelized by the method described in section 2.2, background objects move linearly as shown in Fig.5 (b). In this case, we can estimate the movement of the background objects easily. Thus, simple image complements can be achieved.

3.2.1 Pixels Complement using Spatiotemporal Patches

In this section, we consider image inpainting by using spatiotemporal patches. The spatiotemporal patch is a 3-dimensional patch in the spatiotemporal image

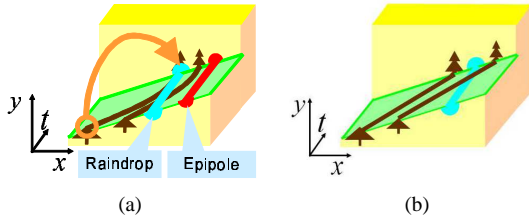


Figure 5: Epipole and raindrop on spatiotemporal slice.

as shown in Fig.6. Note, we can only use past image frames for image inpainting, which are taken before the current image frame, since we cannot predict future images.

Now, let us consider a current image, in which a lacking image pixel exists because of a raindrop. If we consider the image sequence, the lacking pixel can be considered as a point in the 3D spatiotemporal space as shown in Fig.6. In this 3D space, the spatiotemporal patches which include the lacking pixel are considered as template patches. For example, 125 template patches can be considered, if the size of the patch is $5 \times 5 \times 5$. However, the template patches which include future image points cannot be used for image inpainting, and thus only 25 template patches can be selected if the size of the patch is $5 \times 5 \times 5$.

For the image complement, we consider the coherence between a spatiotemporal image S and a reference spatiotemporal image D in the database. The database is constructed from current and past image frames. Let us consider a point p in S and a point q in D . Then, we define the similarity between a spatiotemporal patch W_p in S and a spatiotemporal patch V_q in D as follows:

$$s(W_p, V_q) = e^{-\frac{d(W_p, V_q)}{2\sigma^2}} \quad (6)$$

where σ is the standard deviation of Gaussian image noise on image intensity, and $d(W_p, V_q)$ denotes the L2 distance between W_p and V_q as follows:

$$d(W_p, V_q) = \sum_{(x,y,t)} \|W_p(x,y,t) - V_q(x,y,t)\|^2 \quad (7)$$

Then, the coherence between a spatiotemporal image S and a reference spatiotemporal image D in the database can be defined as follows:

$$Coherence(S|D) = \prod_{p \in S} \max_{q \in D} s(W_p, V_q) \quad (8)$$

The spatiotemporal image S which provides us a maximum coherence is chosen as the complemented spatiotemporal image.

Although the database includes all spatiotemporal images up to the current time, the spatiotemporal patch for p is chosen from patches which are close to

the epipolar line of pixel p . By using this constraint, the search space becomes small, and hence the computational cost of image complement becomes small. Furthermore, errors in the selection of spatiotemporal patch also become small.

Let us describe estimation of pixel value c for lacking point p . The pixel value c of p is determined as coherences for all spatiotemporal templates W_p^i (some spatiotemporal template can be selected for lacking pixel p) become higher. The problem can be represented as minimization of the following equation.

$$\sum_i \omega_p^i (c - c^i)^2 \quad (9)$$

where c^i is a pixel value for p in V^i which is the nearest spatiotemporal patch in the database. The variable ω_p^i is determined as follows:

$$\omega_p^i = \gamma^{-dist_s(W_p^i, V^i)} \quad (10)$$

where γ is a constant and $dist$ is a distance from pixel p to the nearest background pixel in the image. Thus, pixel value c is determined as follows:

$$c = \frac{\sum_i \omega_p^i c^i}{\sum_i \omega_p^i} \quad (11)$$

The complemented image S is updated by using the value c . The database D is also updated so that the database includes complemented images. These processes are iterated until the complemented image converges. The pixel values of lacking pixels are estimated by the process, and thus, the raindrops can be complemented if they are detected, accurately.

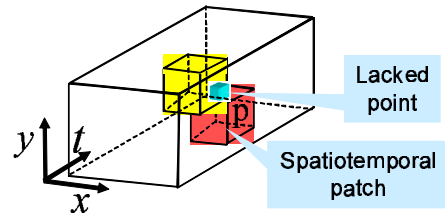


Figure 6: Spatiotemporal patch for complement of lacking point.

4 RAINDROP DETECTION USING IMAGE COMPLEMENT

We next propose a method for detecting raindrops by using the image complement method described in the previous section. We first consider a mask of image as shown in Fig.9 (b). The masked areas are inpainted by the method described in the previous section, and inpainted image (c) can be obtained. Although there

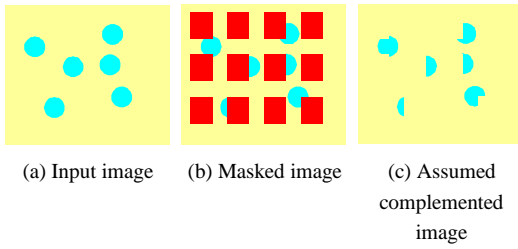


Figure 7: Raindrop detection using masked image.

are some raindrops in the input image, it is not a problem for image complement, since raindrop areas are not used for image complement in general. This is because if the raindrop areas are used for image complement, coherence of spatiotemporal image becomes low, and thus image complements are achieved by using just background areas.

By changing the mask patterns and complementing images, whole image can be inpainted. This method roughly delete raindrops in images, and thus the difference between the obtained image and the input image becomes large at raindrop areas. Therefore, raindrops can be extracted by thresholding the difference image.

By combining the detection method with complement method, we can extract raindrops and eliminate them in images.

5 EXPERIMENT

5.1 Experimental Environment

In this section, we show some experimental results by using the proposed method. In this experiment, a camera is attached near the driver's eyes, and the camera observes the side mirror of the vehicle. The size of the image is 360×240 , and the frame rate of the camera is 30 fps. the speed of the vehicle was about 40 km/h, and 400 image frames were taken. Some example images obtained from the camera are shown in Fig.8. As shown in this figure, raindrops exist in images.

For raindrop detection, 4 patterns of mask image were used, which are shown in Fig.9. Size of spatiotemporal patch is $5 \times 5 \times 5$ and 60 past frames were used for database of image complement.

5.2 Results of Raindrop Detection and Complement

In this section, we show the results of raindrop detection. Fig.10 (a) shows input images for raindrop de-



Figure 8: Input images.

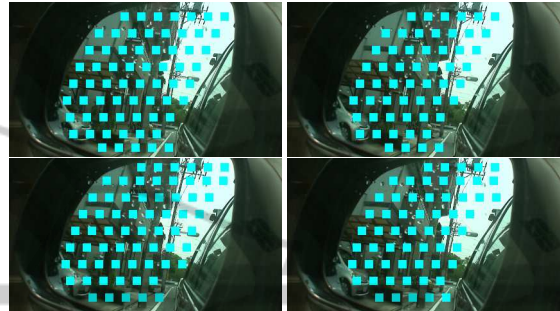


Figure 9: Masking images for raindrop detection.

tection. The raindrops in these images are extracted by using the method proposed in section 4. Fig.10 (b) shows difference between input images and roughly inpainted images, and Fig.10 (c) shows raindrops detected by thresholding the difference image in (b). From these results, most part of raindrops on the mirror can be detected by the proposed method. However, some strong edges are also detected as raindrops. This is because our image complement method becomes unstable around strong edges, and it causes wrong extraction of raindrops.

The extracted raindrops in images were next complemented by using the method proposed in section 3. Fig. 11 shows images generated from the proposed inpainting method. Comparing these images with those in Fig.10 (a), we find that most of the raindrops are inpainted accurately by using the proposed method. Furthermore, strong edge areas extracted as raindrops by mistake were also inpainted properly. Thus, we find that the over extraction of raindrops area does not cause serious problem in our method.

6 CONCLUSIONS

In this paper, we proposed a method for detecting and complementing raindrops on mirrors and windows of vehicles virtually.

We first described a method for complementing raindrops by using the auto-epipolar geometry among sequential images. Since vehicle cameras can be considered as translational cameras in short periods, the auto-epipolar geometry holds and it can be used for

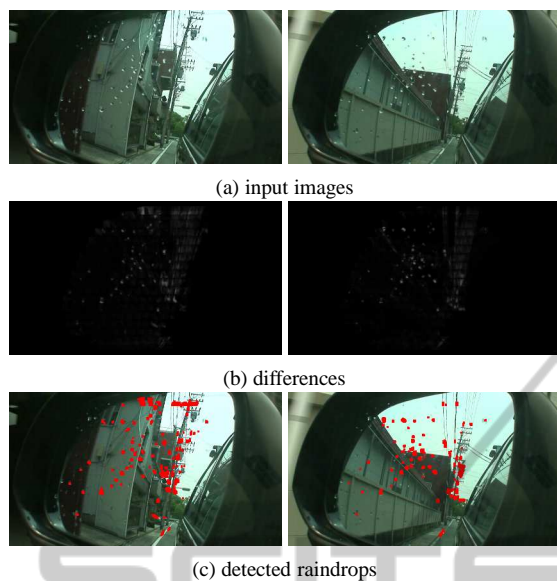


Figure 10: Detection result of raindrops on a side mirror: Input images (a), image differences of virtual image (b) and detection results (c).



Figure 11: Results of raindrop complement. Comparing these images with those in Fig.10 (a), we find the raindrops are inpainted properly by using the proposed method.

complementing images efficiently. The pixel values of lacking pixels are recovered from the coherences of spatiotemporal images.

We next showed that raindrops can be extracted accurately by using the image complement method, and proposed a method for extracting raindrops by complementing masked images. The extracted raindrop areas were inpainted and raindrops are eliminated in images.

The experimental results show that the proposed method works very well for real image sequences with raindrops.

REFERENCES

- Bertalmio, M., Bertozzi, A. L., and Sapiro, G. (2001). Navier-stokes, fluid dynamics, and image and video inpainting. In *Proceedings of the 2001 IEEE Computer Society Conference on Computer Vision and Pattern Recognition (CVPR2001)*, volume 1, pages 355–362.
- Bertalmio, M., Sapiro, G., Caselles, V., and Ballester, C. (2000). Image inpainting. In *ACM Transactions on Computer Graphics (Proceedings of SIGGRAPH2000)*, pages 417–424.
- Bertalmio, M., Vese, L., Sapiro, G., and Osher, S. (2003). Simultaneous structure and texture image inpainting. *IEEE Transactions on Image Processing*, 12(8):882–889.
- Efros, A. and Freeman, W. (2001). Image quilting for texture synthesis and transfer. In *Proc. SIGGRAPH '01*, pages 341–346.
- Hartley, R. and Zisserman, A. (2000). *Multiple View Geometry in Computer Vision*. Cambridge University Press.
- Hase, H., Miyake, K., and Yoneda, M. (1999). Real-time snowfall noise elimination. In *Proceedings of the 1999 IEEE International Conference on Image Processing (ICIP1999)*, volume 2, pages 406–409.
- Kang, S., Chan, T., and Soatto, S. (2002). Inpainting from multiple views. In *Proceedings of the 1st International Symposium on 3D Data Processing Visualization and Transmission*, pages 622–625.
- Kuribayashi, K., Ono, S., Kawasaki, H., and Ikeuchi, K. (2009). Spatio-temporal image filter for removal of obstacles from on-vehicle video data. In *Meeting on Image Recognition and Understanding*, pages 1065–1072.
- Matsushita, Y., Ofek, E., Tang, X., and Shum, H. (2005). Full-frame video stabilization. In *Proceedings of the 2005 IEEE Computer Society Conference on Computer Vision and Pattern Recognition (CVPR2005)*, volume 1, pages 50–57.
- Shen, Y., Lu, F., Cao, X., and Foroosh, H. (2006). Video completion for perspective camera under constrained motion. In *Proceedings of the 18th International Conference on Pattern Recognition (ICPR2006)*, volume 3, pages 63–66.
- Wexler, Y., Shechtman, E., and Irani, M. (2007). Space-time completion of video. *IEEE Transactions on Pattern Analysis and Machine Intelligence*, 29(3):463–476.